

Article

The Effect of Hybrid B₄C and Si₃N₄ Nanoparticles on the Mechanical and Physical Properties of Copper Nanocomposites

Fathi Djouider ¹, Abdulsalam Alhawsawi ^{1,2} , Ezzat Elmoujarkach ¹, Essam Banoqitah ^{1,2} , Omar A. Alammari ³ and Essam B. Moustafa ^{3,*} 

¹ Nuclear Department, Faculty of Engineering, King Abdulaziz University, P.O. Box 80204, Jeddah 21589, Saudi Arabia; fdjouider@kau.edu.sa (F.D.); amalhawsawi@kau.edu.sa (A.A.)

² Center for Training & Radiation Prevention, King Abdulaziz University, P.O. Box 80204, Jeddah 21589, Saudi Arabia

³ Mechanical Engineering Department, Faculty of Engineering, King Abdulaziz University, P.O. Box 80204, Jeddah 21589, Saudi Arabia

* Correspondence: abmostafa@kau.edu.sa

Abstract: This study investigated the effects of reinforcing pure copper with hybrid B₄C and Si₃N₄ nanoparticles on the mechanical and physical properties of the nanocomposite matrix. The composite matrix was prepared using the powder metallurgy (PM) method, allowing uniform nanoparticle dispersion within the copper matrix. The PM method was a practical approach for achieving a homogeneous and good dispersion of the reinforcing particles in the matrix while controlling the porosity and improving the microstructure of the fabricated composite matrix. The addition of B₄C and Si₃N₄ are both very hard and dense materials. When added to a material, they can fill voids and reduce porosity. This can lead to significant improvements in the material's mechanical properties. The study found that adding hybrid B₄C and Si₃N₄ nanoparticles enhanced the microhardness and mechanical properties of the nanocomposites. The improvements in the mechanical and physical properties of such composites containing 5% B₄C were 21.6% and 18.4% higher than the copper base alloy. The findings suggest that including ceramic particles is a viable strategy for enhancing the mechanical characteristics of copper in its pure form. For example, adding 5% B₄C particles to copper resulted in a 23% increase in Young's modulus of the material while reducing electrical conductivity by 4.6%. On the other hand, the hybrid composite Cu/5%B₄C + 2.5%Si₃N₄ showed a 32% improvement in Young's modulus and 71% in the microhardness value compared to the base metal. This makes it a promising option for various engineering applications, such as high-performance electrical contacts and bearings.

Keywords: hybrid composite; copper alloy; B₄C; Si₃N₄; powder metallurgy; mechanical properties; physical properties



Citation: Djouider, F.; Alhawsawi, A.; Elmoujarkach, E.; Banoqitah, E.; Alammari, O.A.; Moustafa, E.B. The Effect of Hybrid B₄C and Si₃N₄ Nanoparticles on the Mechanical and Physical Properties of Copper Nanocomposites. *Metals* **2023**, *13*, 1504. <https://doi.org/10.3390/met13091504>

Academic Editors: Wei Liu and Jürgen Eckert

Received: 30 June 2023

Revised: 13 August 2023

Accepted: 17 August 2023

Published: 22 August 2023



Copyright: © 2023 by the authors. Licensee MDPI, Basel, Switzerland. This article is an open access article distributed under the terms and conditions of the Creative Commons Attribution (CC BY) license (<https://creativecommons.org/licenses/by/4.0/>).

1. Introduction

In recent years, there has been growing interest in developing new materials with enhanced mechanical properties for various engineering applications [1,2]. Metal matrix composites (MMCs) have gained significant attention in recent decades due to their unique properties, such as high strength, stiffness, and wear resistance [3,4]. Among the most commonly used MMCs, copper-based composite materials have gained much attention because of their good mechanical, thermal, and tribological properties [5–8]. One of the most common methods for preparing MMCs is powder metallurgy, a simple and cost-effective synthesis technique. In powder metallurgy, metal powders are mixed with ceramic particles and consolidated under high pressure [9–11]. This process can produce MMCs with a uniform dispersion of ceramic particles in the metal matrix, which can significantly improve the mechanical properties of the material [12–17].

Ceramic particles are often reinforced in MMCs because of their high strength-to-weight ratios [10,18,19]. This can impart good wear resistance, high-temperature durability, and improved mechanical properties to the composite material [20–27]. Several studies have investigated the effect of hybrid nanoparticles on the mechanical properties of pure copper prepared via the powder metallurgy method [28–30]. For instance, A. Moghanian et al. prepared Cu/TiO₂ nanocomposites via mechanical alloying. They found that as the quantity of TiO₂ in the Cu matrix increased, there was a corresponding increase in the hardness and specific electrical resistivity. At the same time, the density of the Cu/TiO₂ nanocomposites decreased [31].

Similarly, Mohammad Hossein Adib et al. prepared Al/Al₂O₃/SiC hybrid nanocomposites via mechanical alloying and reported that the addition of Al₂O₃/SiC nanoparticles with 10% SiC contents significantly enhanced the microhardness and compressive strength of pure copper [32]. The effect of Al₂O₃ ceramic particles on the mechanical properties of copper-based composite materials prepared using mechanical alloying was also investigated [33]. Their findings indicated that incorporating Al₂O₃ particles as function-graded materials (FGM) by changing the formed phase in Cu-Al₂O₃ composites can improve their properties. Electrocorundum was used to limit porosity in the ceramic phase, enhancing mechanical, thermal, and tribological properties. Through ceramic reinforcements, such as carbides and oxides, high strength-to-weight ratios can be achieved, improving wear resistance and durability at high temperatures. Furthermore, internal oxidation and mechanical alloying can achieve the uniform distribution of ceramic particles in copper matrix composites [34–36]. Although ceramic reinforcement particles tend to decrease thermal conductivity, the thermal conductivity of the composites decreases with increasing ARB passes due to the increased number of Al/Cu interfaces [37].

Copper-based metal matrix composites with ceramic reinforcements have exhibited improved mechanical and physical properties, including high-temperature durability, wear resistance, strength-to-weight ratio, and elastic modulus. The studies conducted by Dang Cong et al. and Baradeswaran et al. have demonstrated the effectiveness of incorporating ceramic particles as reinforcements in copper-based metal matrix composites [38]. This work uses pure copper as the base matrix and reinforces it with B₄C and Si₃N₄ ceramic particles to address inherent limitations such as low microhardness and strength. The hybridization of boron carbide and silicon nitride is used to enhance the mechanical and electrical properties of the composite matrix. It is important to carefully consider factors such as particle concentration, distribution, and size to achieve the desired balance between thermal properties and mechanical performance.

2. Materials and Experimental Setup

2.1. Materials

This work uses pure copper powder as the main matrix, boron carbide (B₄C), and silicon nitride Si₃N₄ as reinforcement particles; the particle's size and specifications are illustrated in Table 1. The morphology and particle size of the powders produced were examined using a transmission electron microscope (TEM) of the JEOL JEM-1230 type, operating at 120 kV and equipped with a CCD camera. The milled powders were investigated at different milling times, and the results are presented in Figure 1. The preparation of TEM samples involved the combination of the powder with a minimal quantity of pure ethylene glycol, followed by agitation for approximately 10 min utilizing an ultrasonic device. Subsequently, a small quantity of the suspension was deposited onto a Cu grid coated with carbon and desiccated for 240 s, after which the grid was affixed onto the sample holder of the transmission electron microscope.

2.2. Preparation of the Compositions

The particles were meticulously blended in a tabletop planetary ball mill. Nanocomposites and powders were produced by subjecting them to air-ground conditions at a rotational speed of 500 revolutions per minute (rpm) for durations of 1, 5, 10, 15, and 20 h.

To optimize the outcomes, a quantity of 15 g of the powder mixture was introduced into the containers, ensuring a minimum of 50% vacant space to facilitate the movement of the balls and the transfer of energy to the substance. Additionally, a 1% concentration of stearic acid was employed to prevent the formation of particle aggregates.

Table 1. The copper powder and reinforcement particles specification.

Particles	AVG Particle Size	Purity
Cu	5 μm	99.9%
B ₄ C	800 nm	99.1%
Si ₃ N ₄	38 nm	99.4%

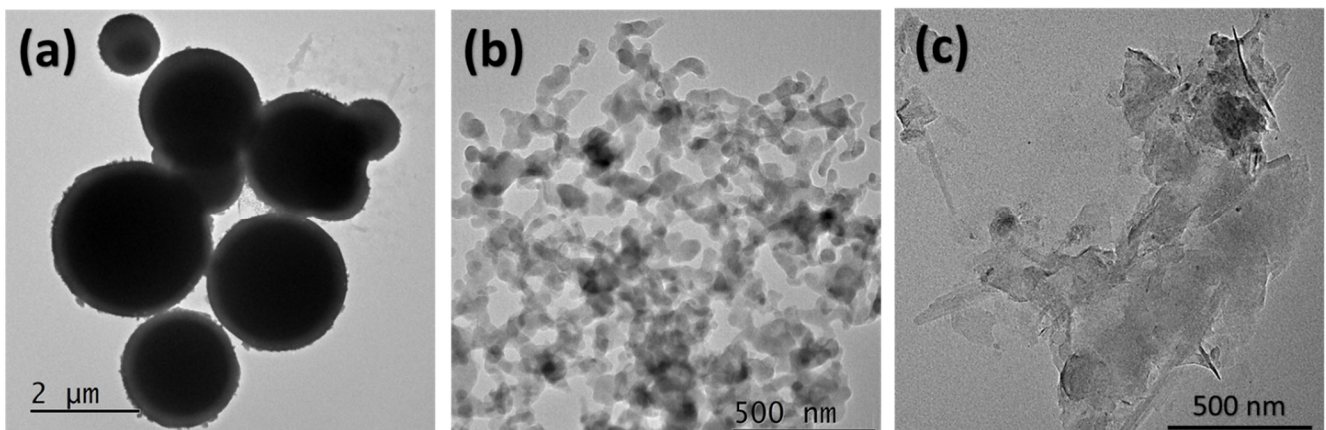


Figure 1. TEM images of the copper powder and reinforcement particles: (a) pure copper powder, (b) silicon nitride nanoparticles (Si₃N₄), and (c) boron carbide (B₄C) particles.

2.3. Powder Synthesis via Mechanical Alloying

In the present investigation, two types of composites were synthesized. The compaction process uses one or two drops of a solution consisting of 100 mL water and 1 mL ethylene glycol added to 5% Cu-B₄C or Cu-Si₃N₄ composites in a mortar to bind the particles together. Subsequently, a disk with dimensions of 1cm across and 4mm by 0.2 mm thick was created by pouring the mixture into a cylinder mold (Figure 2) and pressing it at 200 bar for one minute at room temperature. The sintering process was carried out at a temperature of 850 °C in argon gas for 2 h and a heating rate of 5 °C/min.

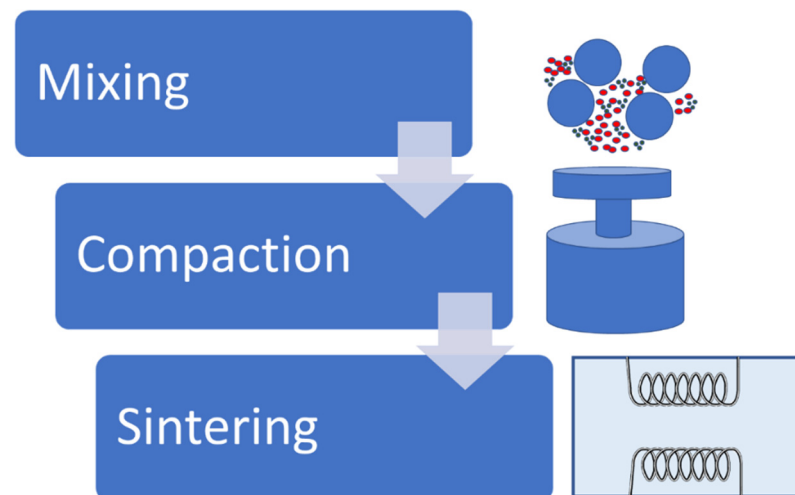


Figure 2. A fabrication process of the copper matrix composite.

The first type is the single composite of 5% Cu- B₄C and Cu-Si₃N₄. The percentage of volume percent was 5%, while the hybrid composite series were as follows:

- Cu/2.5% B₄C + 2.5% Si₃N₄;
- Cu/5% B₄C + 2.5% Si₃N₄;
- Cu/2.5% B₄C + 5% Si₃N₄.

3. Characterization of the Investigated Samples

Microhardness was measured using a Vickers indenter following ASTM B933-09 after applying a load of 1.961 N for 15 s. Compressive tests were conducted according to ASTM E9 using a hydraulic machine. Yield strength, ultimate strength, and elongation were calculated from the stress–strain curve. Ultrasonic velocities and a group of elastic moduli were measured using the pulse-echo method, as described in the literature [39,40]. The microstructure of the samples was examined using a Quanta-FEG250 field emission scanning electron microscope and their chemical composition via energy-dispersive X-ray analysis (FESEM-EDX). The bulk density (BD) and apparent porosity (AP) of each sample were measured using the liquid displacement method and computed using the formulae in Equations (1) and (2) [41]:

$$BD = \frac{W_s - W_d}{W_s - W_i} \times 100 \quad (1)$$

$$AP = \frac{W_d}{W_s - W_i} \times \rho_l \quad (2)$$

where W_d and W_s are the weight of dry and saturated samples in air, respectively, W_i is the weight of immersed sample in liquid, and ρ_l is the density of the liquid.

An electrical properties test was performed using a Keithley 6517B system, and the electrical conductivity of the investigated samples was determined.

A sample's thermal conductivity coefficient, K (W/m·k) can be calculated using the heat flow equation. The apparatus used to measure this coefficient consists of three sections: a heating section, an intermediate section, and a cooling section. The heating and cooling sections are radially isolated from each other to minimize heat loss. Thermocouples are evenly distributed throughout the heated and cooled sections to measure the temperature difference. The intermediate section is coated with an insulating substance to prevent heat loss. The spacer is tightly clamped between the heated and cooled sections. Thermal paste is applied to both surfaces to ensure optimal contact and heat transfer. The cooling water flow rate is set to 1.5 L/min by withdrawing 500 mL of water every 20 s. The calibrated material in full contact with the heated section transfers heat linearly to the sample.

Thermal conductivity is directly measured in a steady-state condition, where heat flow is unidirectional. Fourier's law describes the heat transfer rate in a sample, and Equation (3) is used to calculate the conduction heat flow in one dimension, where Q is the heat transfer rate in the x -direction, k is the sample material's thermal conductivity, A is the cross-sectional area of the sample normal to the x -direction, and dT/dx is the temperature gradient in the x -direction.

$$Q = -kA \frac{dT}{dX} \quad (3)$$

4. Results and Discussion

4.1. Porosity and Microstructure Observation

The effect of reinforcing pure copper with B₄C and Si₃N₄ particles prepared via powder metallurgy composites on porosity and microstructure observation is investigated. Both B₄C and Si₃N₄ particles significantly affected the porosity and microstructure of the pure copper composite material. The SEM images depicted in Figure 3 demonstrate that the pores generated by employing powder metallurgy (PM) techniques are minimal owing to the effective compaction and appropriate percentage of reinforcement volume. There are no defects or significant pores in the investigated samples. The addition of B₄C and

Si_3N_4 particles led to a reduction in porosity and an improvement in the microstructure of the material. The observed reduction in porosity was attributed to the homogeneous distribution of reinforcing particles achieved through the powder metallurgy method. In addition, the microstructure of the composites showed that both B_4C and Si_3N_4 particles were well dispersed within the copper matrix.

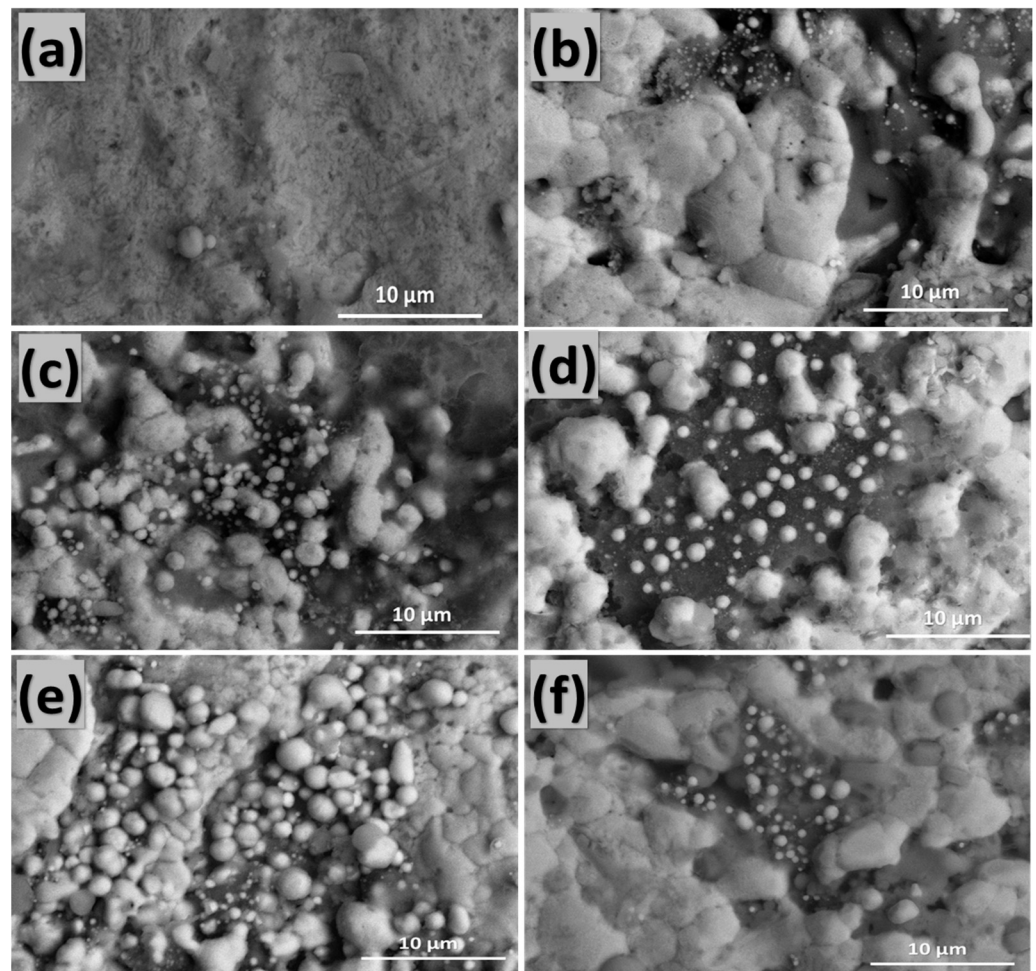


Figure 3. SEM images of the examined samples: (a) the microstructural characterization of the pure copper, (b) mono-composite 5% Cu- B_4C , (c) mono-composite Cu/5% Si_3N_4 , (d) hybrid composite Cu/2.5% B_4C + 2.5% Si_3N_4 , (e) hybrid composite Cu/5% B_4C + 2.5% Si_3N_4 , and (f) hybrid composite Cu/2.5% B_4C + 5% Si_3N_4 .

Figure 4 shows that the base alloy had the lowest apparent porosity of all the investigated samples. The base alloy has a relatively uniform structure with few defects or voids. However, when reinforcement particles were added, the apparent porosity increased. The reinforcement particles distribute the material's structure, creating more space. The error bars in the apparent porosity and the bulk density of the investigated samples represent the uncertainty in the measurement. This uncertainty can be caused by many factors, such as the accuracy of the equipment used to measure the porosity, the variation in the sample size, and the variability of the material itself.

4.2. Physical Properties

The results depicted in Figure 5 indicate that incorporating reinforcement nanoparticles, namely B_4C or Si_3N_4 , leads to a notable decrease in the bulk density of the specimens under investigation. In the case of a hybrid composite from a copper base matrix reinforced with Si_3N_4 and B_4C nanoparticles, the density of the composite can be reduced by increas-

ing the volume fraction of the nanoparticles. This is because the nanoparticles are very light and will occupy space without significantly increasing the weight of the composite. However, if the volume fraction of the nanoparticles is too high, the composite may become brittle. The density of the composite can also be reduced by creating defects during processing. This can be performed using a high-energy milling process or by introducing air bubbles into the composite during processing. However, defects can also weaken the composite, so it is important to balance reducing the density with maintaining the strength of the composite's structure.

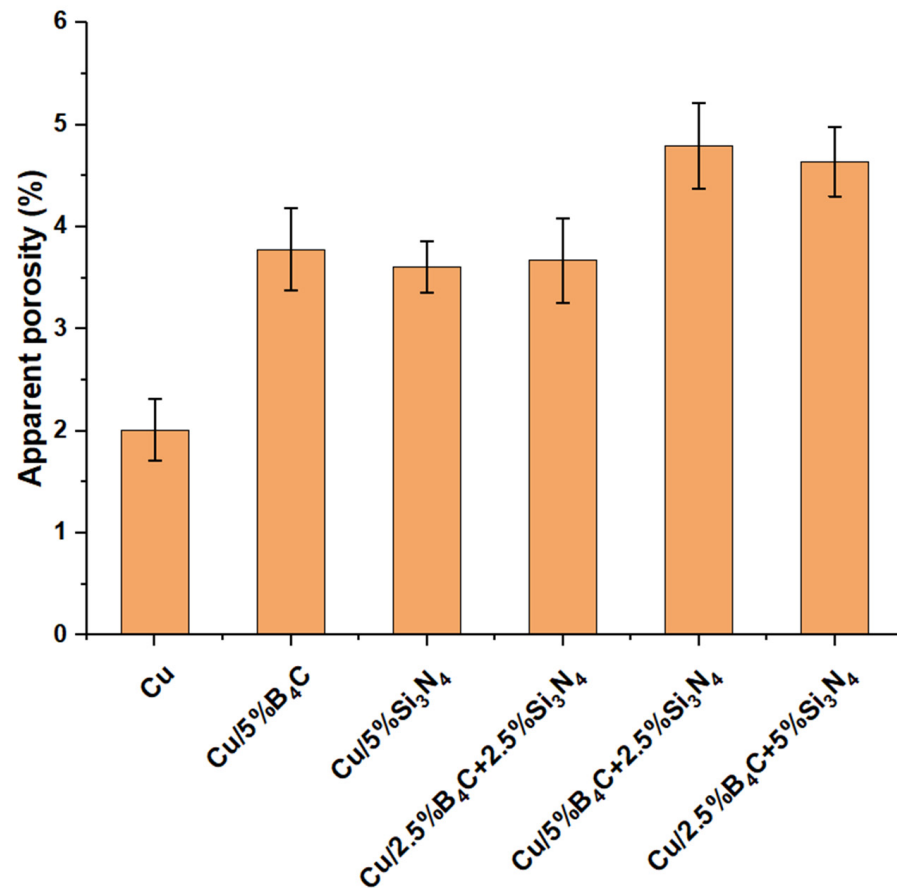


Figure 4. Mean apparent porosity of the composites samples.

It is evident that the incorporation of 5% of B₄C in the mono-composite specimens resulted in a 5.5% increase in bulk density. Similarly, adding 5 volume percent of Si₃N₄ led to a 4.9% enhancement in bulk density. Conversely, incorporating hybrid composites comprising 2.5% of B₄C and 2.5% of Si₃N₄ has yielded outcomes almost comparable to those of the mono-composite with a 5.2% enhancement. Adding 5% of B₄C and 2.5 vol % of Si₃N₄ has yielded the most significant improvement results, resulting in a 9% reduction in bulk density. Altering the composition to include 2.5% of B₄C and 5% of Si₃N₄ has resulted in superior outcomes compared to the mono-composite, with an 8.4% improvement in bulk density. Incorporating hybrid nanocomposites containing 5% of B₄C and 2.5% of Si₃N₄ has yielded the most favorable outcomes, as evidenced by a 9% increase in bulk density. As depicted in Figure 6 and delineated in Table 2, it is evident that the variance between the bulk and theoretical density is negligible, exhibiting a 2.1% dissimilarity in Cu and 6.1% in Cu, 5% B₄C + 2.5% Si₃N₄. This is the reason why the bulk density decreases with the increase in B₄C at a fixed percentage of Si₃N₄ in a copper base metal reinforced with Si₃N₄ and B₄C.

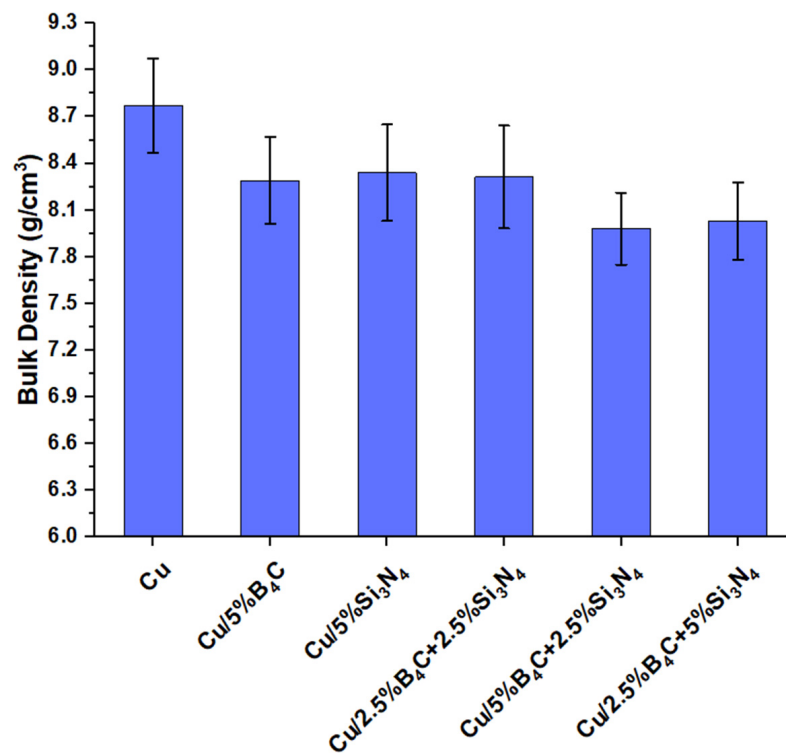


Figure 5. Bulk density outputs for mono and hybrid composites.

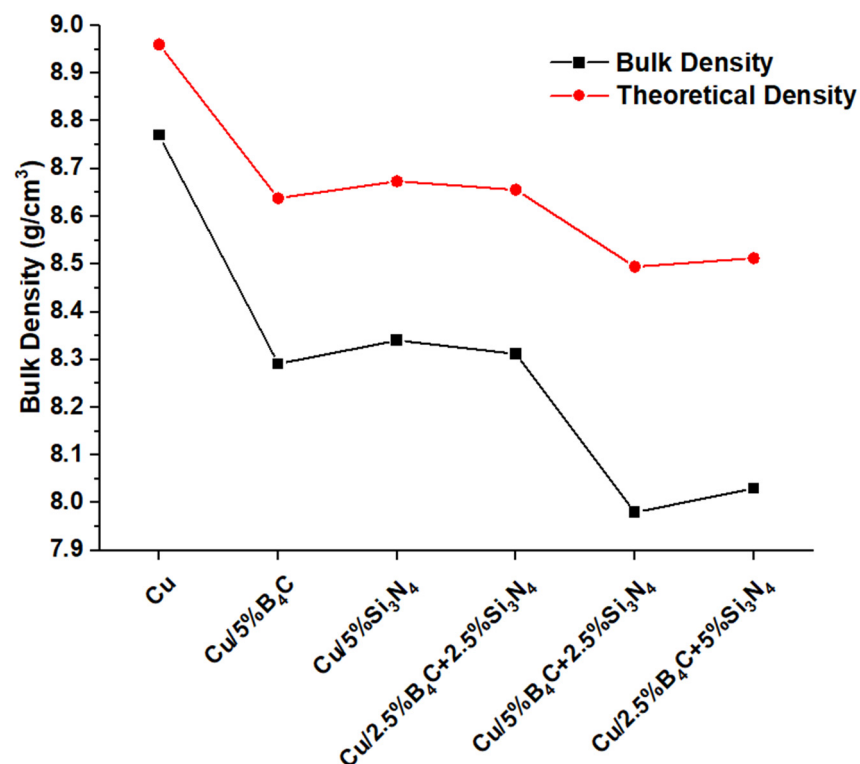


Figure 6. Comparison between bulk and theoretical density.

The incorporation of B₄C in the composite leads to a significant increase in volume without a significant increase in weight. The density of the composite material decreases because B₄C has a lower bulk modulus than Si₃N₄. This means that B₄C is more compliant than Si₃N₄, which allows it to deform more easily. Voids or pores in the composite material

can also decrease its density. Additionally, the interfacial properties of B₄C and copper are not as good as those of Si₃N₄ and copper. This can lead to less-than-optimal interfaces between the B₄C particles and the copper matrix. Finally, the inclusion of voids or pores within the composite material can further decrease its overall density.

Table 2. Comparison between bulk and theoretical density.

Samples	Bulk Density (g/cm ³)	Theoretical Density (g/cm ³)	Difference %
Cu	8.77	8.96	2.12054
Cu/5% B ₄ C	8.291	8.638	4.01713
Cu/5% Si ₃ N ₄	8.34	8.6735	3.84505
Cu/2.5% B ₄ C + 2.5% Si ₃ N ₄	8.312	8.65575	3.97135
Cu/5% B ₄ C + 2.5% Si ₃ N ₄	7.98	8.49475	6.05963
Cu/2.5% B ₄ C + 5% Si ₃ N ₄	8.03	8.5125	5.66814

4.3. Electrical Conductivity

The exceptional electrical conductivity of pure copper has made it a popular choice for various electrical and electronic applications. The practical applications of pure copper are limited in certain fields due to its low microhardness and poor wear resistance. To solve these problems, the amount of B₄C and Si₃N₄ particles is the most important factor that controls the overall properties of the composite. The results showed that adding B₄C and Si₃N₄ particles made the pure copper matrix composite less conductive. However, the decrease in electrical conductivity was minimal for low-loading fractions of the reinforcing particles. Also, the study found that as the amount of B₄C particles increased, the composite's ability to conduct electricity decreased, which is in line with [42]. Based on these results, adding B₄C and Si₃N₄ particles to a pure copper matrix composite may make the microhardness and mechanical properties of the composite better, but it may also make the composite less good at conducting electricity. Optimizing the amount and size of the reinforcing particles facilitates striking a balance between electrical conductivity and improving mechanical properties. From the previous results, the B₄C and Si₃N₄ particles reduced the electrical conductivity by 4.8% and 11.9%, respectively; thus, the results revealed that the current investigation improved the electrical conductivity compared with the previous studies. In a study by Singh et al., they found that incorporating hybrid ceramic reinforcement particles and B₄C with 5% v contents into a copper matrix reduced the electrical conductivity by 62% with respect to the copper base matrix [43]. As shown in Figure 7, the 2.5% vol. of the hybrid B₄C and Si₃N₄ particles results in minor losses in the electrical conductivity compared with the other hybrid percentage ratios.

4.4. Thermal Conductivity

Adding ceramic particles such as B₄C and Si₃N₄ to a pure copper matrix alters thermal properties by enhancing thermal conductivity and the thermal expansion coefficient. The improvement in thermal conductivity can be attributed to the higher thermal conductivity of B₄C and Si₃N₄ compared to copper and the increased interfacial thermal conductivity between the particles and matrix. The enhancement of thermal conductivity also depends on particle size, concentration, and distribution. These composites show lower thermal conductivity than pure copper due to the impurities in the ceramic particles. However, it was found that thermal conductivity enhancement is affected by particle size and distribution.

Furthermore, adding ceramic particles to copper may reduce ductility and ultimate tensile strength due to the inherent brittleness of the ceramic particles. Therefore, the optimal concentration and distribution of ceramic particles must be carefully considered to achieve the desired balance between thermal properties and mechanical performance. In addition, it should be noted that the particle size may adversely affect the composites' ther-

mal conductivity. Although the reduction in the thermal conductivity is minor, as shown in Figure 8, the hybrid Cu/2.5% B₄C + 2.5% Si₃N₄ achieved the optimum ceramic percentage to enhance the thermal conductivity without decreasing the mechanical properties.

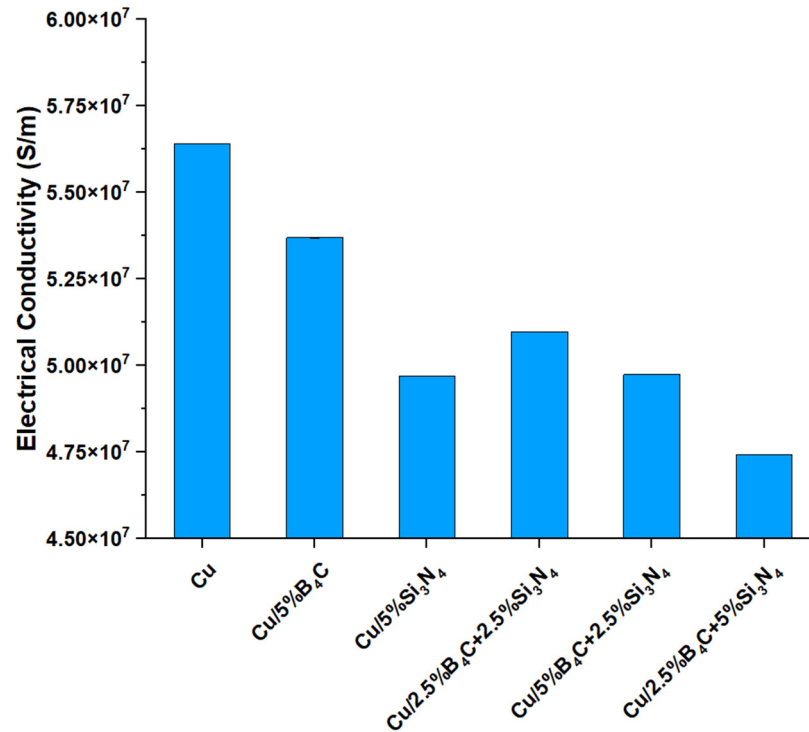


Figure 7. Electrical conductivity of the investigated samples.

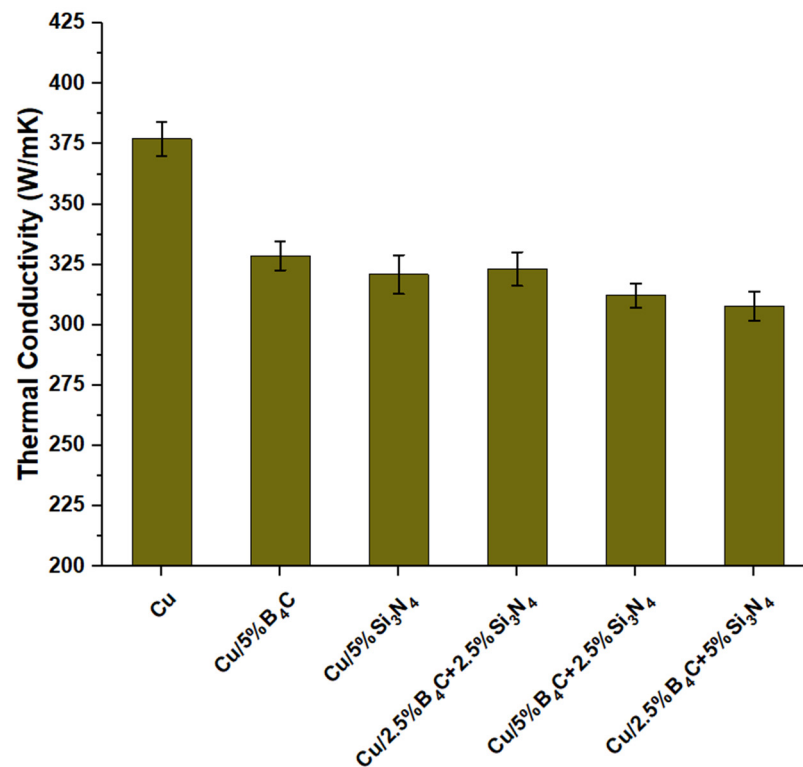


Figure 8. Thermal conductivity of the investigated samples.

In general, a composite's electrical and thermal conductivity will increase as the particle size decreases. However, the effect of particle size on electrical and thermal conductivity is not linear. There is a point when the particle size becomes so small that the electrical and thermal conductivity decreases. This is because the small particles can start interfering with each other, making it more difficult for electrons or heat to flow. The chemical composition of the composite can also affect its electrical and thermal conductivity. For example, adding B_4C to a copper matrix can significantly increase the electrical and thermal conductivity of the composite. This is because B_4C is a very hard and dense material, which makes it a good conductor of electricity and heat. The interplay between particle size, distribution, and chemical composition is complex and difficult to predict. However, understanding the basic principles makes it possible to design composites with improved electrical and thermal conductivity.

4.5. Mechanical Properties

Figure 9a illustrates the microhardness characteristics of the specimens being examined. According to the data presented in the figure, it can be observed that Cu displays the minimum value of the microhardness measurement. The inclusion of reinforcement nanoparticles, specifically B_4C or Si_3N_4 , significantly enhances the microhardness properties of the analyzed samples. The findings suggest that incorporating 5 volume percent of boron carbide (B_4C) into the monolithic composite specimens led to a notable enhancement in their microhardness, exhibiting a rise of 41.1%. Likewise, incorporating 5% volume of silicon nitride (Si_3N_4) yielded a 26.3% augmentation in the microhardness.

On the other hand, integrating hybrid composites consisting of 2.5 volume percent of B_4C and 2.5 volume percent of Si_3N_4 produces results similar to those of the single composite. The single composite shows an improvement of 33.7%. Adding 5 volume percent of B_4C and 2.5 volume percent of Si_3N_4 has substantially improved the microhardness properties, demonstrating a remarkable increase of 69.7%. In contrast, the incorporation of 2.5% of B_4C and 5% of Si_3N_4 into the composition has yielded more favorable results than the monolithic composite, exhibiting a significant increase in microhardness by 47.2%. Utilizing hybrid nanocomposites comprising 5% of B_4C and 2.5% of Si_3N_4 has resulted in favorable results, as demonstrated by a 69.7% enhancement in the microhardness characteristics.

Figure 9b illustrates a significant enhancement in Young's modulus of the specimens under investigation following the integration of reinforcement nanoparticles, namely B_4C or Si_3N_4 . The findings suggest that 5 vol % of B_4C in the mono-composite specimens significantly increased Young's modulus by 21.5%. Introducing 5 volume percent of Si_3N_4 led to a notable enhancement in Young's modulus, exhibiting a rise of 16.3%. On the other hand, integrating hybrid composites consisting of 2.5% B_4C and 2.5% Si_3N_4 produces similar improvement results as the nanocomposite, which is equivalent to 17.9%. Adding 5 volume percent of B_4C and 2.5 volume percent of Si_3N_4 has resulted in the most favorable improvement outcomes, demonstrating a 29.7% increase in Young's modulus, consistent with [44]. Incorporating 2.5 vol % of B_4C and 5 vol % of Si_3N_4 into the composition has improved outcomes compared to the monolithic composite. This has resulted in a 25.5% increase in Young's modulus. The use of hybrid nanocomposites, comprising 5% volume of B_4C and 2.5% volume of Si_3N_4 , has yielded highly favorable outcomes. This composition has shown a notable improvement in Young's modulus, with a 29.7% increase.

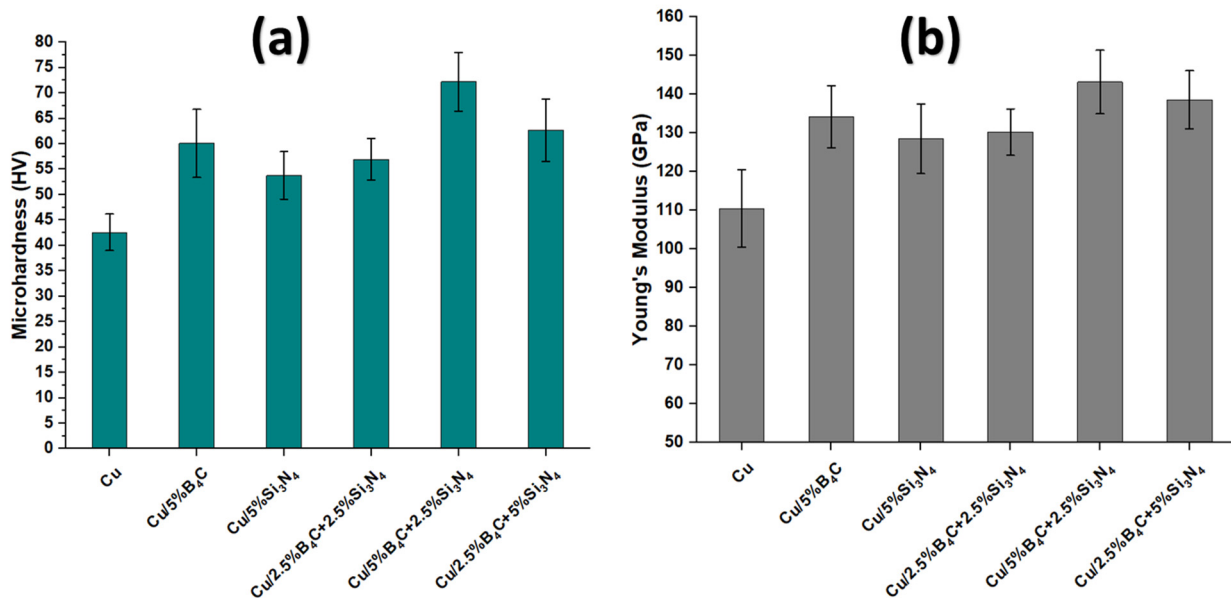


Figure 9. Mechanical properties of the fabricated samples: (a) microhardness, (b) Young's modulus.

5. Conclusions

- The reinforcement of pure copper with hybrid nanoparticles prepared via the mechanical alloying method can significantly improve its mechanical and physical properties. The type and concentration of nanoparticles play a crucial role in determining the mechanical properties of the composites. Therefore, it is very important to optimize the nanoparticle concentration and processing parameters to achieve maximum improvement in the mechanical properties of pure copper.
- Powder metallurgy is an effective approach for producing homogeneous and well-dispersed composites. It can evenly distribute reinforcing particles in the matrix, manage porosity, and improve composite microstructure. B₄C and Si₃N₄ particles reduced porosity and consequently improved mechanical and physical properties.
- The electrical and thermal conductivity of copper-based composites were less than the base alloy by 4.6% and 13%, respectively. However, in this study, the thermal and electrical conductivity of the composites did not decrease significantly compared to the previous studies. This suggests that adding B₄C and Si₃N₄ particles to a pure copper matrix using powder metallurgy composites is an effective approach for maintaining desirable electrical and thermal conductivity.
- The hybrid composite of copper reinforced with 5% boron carbide and 2.5% silicon nitride showed a significant increase of 32% in Young's modulus and a substantial improvement of 71% in microhardness compared to the pure base metal.

Author Contributions: Conceptualization, O.A.A. and E.B.M.; methodology, E.B.M.; software, O.A.A.; validation, F.D., A.A. and E.E.; formal analysis, E.B.M.; investigation, E.B.M.; resources, F.D.; data curation, E.E.; writing—original draft preparation, E.B.M.; writing—review and editing, E.B.M. and E.B.; visualization, F.D.; supervision, A.A.; project administration, E.B.M.; funding acquisition, F.D. All authors have read and agreed to the published version of the manuscript.

Funding: This research was funded by Ministry of Education in Saudi Arabia, grant number (IFPRC-64-135-2020). And The APC was funded by all authors.

Data Availability Statement: Not applicable.

Acknowledgments: The authors extend their appreciation to the Deputyship of Research & Innovation, Ministry of Education in Saudi Arabia for funding this research work through the project number (IFPRC-64-135-2020), and to the King Abdulaziz University, Jeddah, Saudi Arabia.

Conflicts of Interest: The authors declare no conflict of interest.

References

1. Tabandeh-Khorshid, M.; Ajay, K.; Omrani, E.; Kim, C.; Rohatgi, P. Synthesis, characterization, and properties of graphene reinforced metal-matrix nanocomposites. *Compos. Part B Eng.* **2020**, *183*, 107664. [[CrossRef](#)]
2. Abdizadeh, H.; Ebrahimifard, R.; Baghchesara, M.A. Investigation of microstructure and mechanical properties of nano MgO reinforced Al composites manufactured by stir casting and powder metallurgy methods: A comparative study. *Compos. Part B Eng.* **2014**, *56*, 217–221. [[CrossRef](#)]
3. Giroto, F.A.; Majidi, A.P.; Chou, T.W. Metal Matrix Composites. In *Encyclopedia of Physical Science and Technology*, 3rd ed.; Meyers, R.A., Ed.; Academic Press: New York, NY, USA, 2003; pp. 485–493.
4. Bedolla-Becerril, E.; Garcia-Guerra, J.; Lopez-Morelos, V.H.; Garcia-Renteria, M.A.; Falcon-Franco, L.A.; Martinez-Landeros, V.H.; Garcia-Villarreal, S.; Flores-Villaseñor, S.E. Tribological Behaviour of Al-2024/TiC Metal Matrix Composites. *Coatings* **2023**, *13*, 77. [[CrossRef](#)]
5. Şap, S.; Uzun, M.; Usca, Ü.A.; Pimenov, D.Y.; Giasin, K.; Wojciechowski, S. Investigation on microstructure, mechanical, and tribological performance of Cu base hybrid composite materials. *J. Mater. Res. Technol.* **2021**, *15*, 6990–7003. [[CrossRef](#)]
6. Pan, Y.; Lu, X.; Volinsky, A.A.; Liu, B.; Xiao, S.; Zhou, C.; Li, Y.; Chen, M.; Qu, X. Tribological and mechanical properties of copper matrix composites reinforced with carbon nanotube and alumina nanoparticles. *Mater. Res. Express* **2019**, *6*, 116524. [[CrossRef](#)]
7. Lakshmikanthan, A.; Angadi, S.; Malik, V.; Saxena, K.K.; Prakash, C.; Dixit, S.; Mohammed, K.A. Mechanical and Tribological Properties of Aluminum-Based Metal-Matrix Composites. *Materials* **2022**, *15*, 6111. [[CrossRef](#)] [[PubMed](#)]
8. Alazwari, M.A.; Moustafa, E.B.; Khoshaim, A.B.; Taha, M.A. Mechanical and wear evolution of in situ synthesized Ti–Cu alloy matrix hybrid composite reinforced by low-cost activated carbon and silica fume waste ceramic for industrial applications. *J. Mater. Res. Technol.* **2023**, *22*, 2284–2296. [[CrossRef](#)]
9. Neikov, O.D. Chapter 3—Mechanical Alloying. In *Handbook of Non-Ferrous Metal Powders*; Neikov, O.D., Naboychenko, S.S., Murashova, I.V., Gopienko, V.G., Frishberg, I.V., Lotsko, D.V., Eds.; Elsevier: Oxford, UK, 2009; pp. 63–79.
10. Suryanarayana, C. Mechanical Alloying: A Novel Technique to Synthesize Advanced Materials. *Research* **2019**, *2019*, 4219812. [[CrossRef](#)]
11. Suryanarayana, C. Mechanical alloying: A critical review. *Mater. Res. Lett.* **2022**, *10*, 619–647. [[CrossRef](#)]
12. Awotunde, M.A.; Adegbenjo, A.O.; Obadele, B.A.; Okoro, M.; Shongwe, B.M.; Olubambi, P.A. Influence of sintering methods on the mechanical properties of aluminium nanocomposites reinforced with carbonaceous compounds: A review. *J. Mater. Res. Technol.* **2019**, *8*, 2432–2449. [[CrossRef](#)]
13. Reddy, M.P.; Manakari, V.; Parande, G.; Shakoore, R.A.; Mohamed, A.M.A.; Gupta, M. Structural, mechanical and thermal characteristics of Al-Cu-Li particle reinforced Al-matrix composites synthesized by microwave sintering and hot extrusion. *Compos. Part B Eng.* **2019**, *164*, 485–492. [[CrossRef](#)]
14. Kallip, K.; Babu, N.K.; AlOgab, K.A.; Kollo, L.; Maeder, X.; Arroyo, Y.; Leparoux, M. Microstructure and mechanical properties of near net shaped aluminium/alumina nanocomposites fabricated by powder metallurgy. *J. Alloys Compd.* **2017**, *714*, 133–143. [[CrossRef](#)]
15. Schramm Deschamps, I.; dos Santos Avila, D.; Vanzuita Piazero, E.; Dudley Cruz, R.C.; Aguilar, C.; Klein, A.N. Design of In Situ Metal Matrix Composites Produced by Powder Metallurgy—A Critical Review. *Metals* **2022**, *12*, 2073. [[CrossRef](#)]
16. AbuShanab, W.S.; Moustafa, E.B.; Ghandourah, E.; Taha, M.A. Effect of graphene nanoparticles on the physical and mechanical properties of the Al2024-graphene nanocomposites fabricated by powder metallurgy. *Results Phys.* **2020**, *19*, 103343. [[CrossRef](#)]
17. Wang, Y.; Tayyebi, M.; Tayebi, M.; Yarigaravesh, M.; Liu, S.; Zhang, H. Effect of whisker alignment on microstructure, mechanical and thermal properties of Mg-SiCw/Cu composite fabricated by a combination of casting and severe plastic deformation (SPD). *J. Magnes. Alloys* **2023**, *11*, 966–980. [[CrossRef](#)]
18. Tschopp, M.A.; Murdoch, H.A.; Kecskes, L.J.; Darling, K.A. “Bulk” Nanocrystalline Metals: Review of the Current State of the Art and Future Opportunities for Copper and Copper Alloys. *JOM* **2014**, *66*, 1000–1019. [[CrossRef](#)]
19. Chaubey, A.K.; Scudino, S.; Khoshkhoo, M.S.; Prashanth, K.G.; Mukhopadhyay, N.K.; Mishra, B.K.; Eckert, J. Synthesis and Characterization of NanocrystallineMg-7.4%Al Powders Produced by Mechanical Alloying. *Metals* **2013**, *3*, 58–68. [[CrossRef](#)]
20. Prakash, D.S.; Balaji, V.; Rajesh, D.; Anand, P.; Karthick, M. Experimental investigation of nano reinforced aluminium based metal matrix composites. *Mater. Today Proc.* **2022**, *54*, 852–857. [[CrossRef](#)]
21. Sam, M.; Radhika, N. Influence of carbide ceramic reinforcements in improving tribological properties of A333 graded hybrid composites. *Def. Technol.* **2022**, *18*, 1107–1123. [[CrossRef](#)]
22. Abushanab, W.S.; Moustafa, E.B.; Melaibari, A.A.; Kotov, A.D.; Mosleh, A.O. A Novel Comparative Study Based on the Economic Feasibility of the Ceramic Nanoparticles Role’s in Improving the Properties of the AA5250 Nanocomposites. *Coatings* **2021**, *11*, 977. [[CrossRef](#)]
23. Khelge, S.; Kumar, V.; Shetty, V.; Kumaraswamy, J. Effect of reinforcement particles on the mechanical and wear properties of aluminium alloy composites: Review. *Mater. Today Proc.* **2022**, *52*, 571–576. [[CrossRef](#)]
24. Kan, W.H.; Huang, S.; Proust, G.; Bhatia, V.; Chang, L.; Lucey, T.; Tang, X.; Cairney, J.M. Improving metal-ceramic systems subjected to sliding contact by reinforcing the metallic counterpart with ceramic particles. *Wear* **2020**, *452–453*, 203311. [[CrossRef](#)]

25. Van Dong, P.; Phan, N.H.; Patil, S.; Shirguppikar, S.; Kalel, S.; Thanh, L.T.P.; Hien, D.M. Effect of boron carbide reinforcement on properties of stainless-steel metal matrix composite for nuclear applications. *J. Mech. Behav. Mater.* **2022**, *31*, 390–397. [[CrossRef](#)]
26. Moustafa, E.B.; Mikhaylovskaya, A.V.; Taha, M.A.; Mosleh, A.O. Improvement of the microstructure and mechanical properties by hybridizing the surface of AA7075 by hexagonal boron nitride with carbide particles using the FSP process. *J. Mater. Res. Technol.* **2022**, *17*, 1986–1999. [[CrossRef](#)]
27. Moustafa, E.B.; Abushanab, W.S.; Melaibari, A.A.; Yakovtseva, O.A.; Mosleh, A. The Effectiveness of Incorporating Hybrid Reinforcement Nanoparticles in the Enhancement of the Tribological Behavior of Aluminum Metal Matrix Composites. *JOM* **2021**, *73*, 4338–4348. [[CrossRef](#)]
28. Singh, K.; Khanna, V.; Chaudhary, V. Effect of Hybrid Reinforcements on the Mechanical Properties of Copper Nanocomposites. *ECS J. Solid State Sci. Technol.* **2022**, *11*, 097001. [[CrossRef](#)]
29. Ramkumar, K.R.; Radhika, N.; Sivasankaran, S.; Kim, H.S. Evolution of microstructure and mechanical properties of [Cu–10Ni]–Si₃N₄ nanocomposites developed using mechanical alloying and spark plasma sintering. *J. Alloys Compd.* **2022**, *899*, 163319. [[CrossRef](#)]
30. Yang, L.; Jiang, X.; Sun, H.; Shao, Z.; Fang, Y.; Shu, R. Effects of alloying, heat treatment and nanoreinforcement on mechanical properties and damping performances of Cu–Al-based alloys: A review. *Nanotechnol. Rev.* **2021**, *10*, 1560–1591. [[CrossRef](#)]
31. Moghanian, A.; Sharifianjazi, F.; Abachi, P.; Sadeghi, E.; Jafarikhorami, H.; Sedghi, A. Production and properties of Cu/TiO₂ nano-composites. *J. Alloys Compd.* **2017**, *698*, 518–524. [[CrossRef](#)]
32. Adib, M.H.; Abedinzadeh, R. Study of mechanical properties and wear behavior of hybrid Al/(Al₂O₃+SiC) nanocomposites fabricated by powder technology. *Mater. Chem. Phys.* **2023**, *305*, 127922. [[CrossRef](#)]
33. Strojny-Nędza, A.; Pietrzak, K.; Węglewski, W. The Influence of Al₂O₃ Powder Morphology on the Properties of Cu–Al₂O₃ Composites Designed for Functionally Graded Materials (FGM). *J. Mater. Eng. Perform.* **2016**, *25*, 3173–3184. [[CrossRef](#)]
34. Nirala, A.; Soren, S.; Kumar, N.; Kaushal, D.R. A comprehensive review on mechanical properties of Al–B₄C stir casting fabricated composite. *Mater. Today Proc.* **2020**, *21*, 1432–1435. [[CrossRef](#)]
35. Shetty, R.P.; Mahesh, T.S.; Ali, Z.; Veerasha, G.; Nagara, M. Studies on mechanical behaviour and tensile fractography of boron carbide particles reinforced Al8081 alloy advanced metal composites. *Mater. Today Proc.* **2022**, *52*, 2115–2120. [[CrossRef](#)]
36. Huang, J.; Tayyebi, M.; Assari, A.H. Effect of SiC particle size and severe deformation on mechanical properties and thermal conductivity of Cu/Al/Ni/SiC composite fabricated by ARB process. *J. Manuf. Process.* **2021**, *68*, 57–68. [[CrossRef](#)]
37. Luo, J.; Khattejad, R.; Assari, A.; Tayyebi, M.; Hamawandi, B. Microstructure, Mechanical and Thermal Properties of Al/Cu/SiC Laminated Composites, Fabricated by the ARB and CARB Processes. *Crystals* **2023**, *13*, 354. [[CrossRef](#)]
38. Cong, D.; Huimin, L.; Shan, F.; Yuan, Q.; Qilong, H.; Jiachen, J. Effect of La₂O₃ addition on copper matrix composites reinforced with Al₂O₃ ceramic particles. *Mater. Res. Express* **2019**, *6*, 106312. [[CrossRef](#)]
39. Abushanab, W.S.; Moustafa, E.B.; Youness, R.A. Evaluation of the dynamic behavior, elastic properties, and in vitro bioactivity of some borophosphosilicate glasses for orthopedic applications. *J. Non Cryst. Solids* **2022**, *586*, 121539. [[CrossRef](#)]
40. Abulyazied, D.E.; Alturki, A.M.; Youness, R.A.; Abomostafa, H.M. Synthesis, Structural and Biomedical Characterization of Hydroxyapatite/Borosilicate Bioactive Glass Nanocomposites. *J. Inorg. Organomet. Polym. Mater.* **2021**, *31*, 4077–4092. [[CrossRef](#)]
41. Taha, M.A.; Zawrah, M.F.; Abomostafa, H.M. Fabrication of Al/Al₂O₃/SiC/graphene hybrid nanocomposites from Al-dross by powder metallurgy: Sinterability, mechanical and electrical properties. *Ceram. Int.* **2022**, *48*, 20923–20932. [[CrossRef](#)]
42. Dİler, E.A. Comparison of the effects of microwave and spark plasma sintering on the electrical, thermal, and mechanical properties of Cu–LaB₆ nanocomposites. *Gümüşhane Üniversitesi Fen Bilim. Enstitüsü Derg.* **2021**, *11*, 1282–1294. [[CrossRef](#)]
43. Singh, M.K.; Gautam, R.K. Structural, Mechanical, and Electrical Behavior of Ceramic-Reinforced Copper Metal Matrix Hybrid Composites. *J. Mater. Eng. Perform.* **2019**, *28*, 886–899. [[CrossRef](#)]
44. Wang, Y.; Huang, P.; Liu, S.; Tayyebi, M.; Tayebi, M. Microstructural evolution, shielding effectiveness, and the ballistic response of Mg/Al7075/B₄C/Pb composite produced by combination of coating and severe plastic deformation (SPD) processes. *J. Manuf. Process.* **2022**, *84*, 977–985. [[CrossRef](#)]

Disclaimer/Publisher’s Note: The statements, opinions and data contained in all publications are solely those of the individual author(s) and contributor(s) and not of MDPI and/or the editor(s). MDPI and/or the editor(s) disclaim responsibility for any injury to people or property resulting from any ideas, methods, instructions or products referred to in the content.